Supporting Information

Anderson et al. 10.1073/pnas.1216398109

SI Methods

Generation of RNAi Vectors. All transfection and infection experiments for shRNA expression were performed with the same lentiviral vector system (see Fig. 1*B* for the schematic diagram of vector). Lentiviral vector (L309) that includes the RNA-polymerase III promoter human H1 was constructed based on the standard lentiviral backbone vector described previously (1). The H1 promoter was cloned into the PacI site upstream of the ubiquitin C promoter and endowed with a multiple cloning sites downstream. Gene-specific targeting shRNA sequences were cloned into the XhoI-XbaI site downstream of H1 promoter (for list of oligonucleotides, see Tables S2–S4). A mCherry expression sequence was inserted downstream of the ubiquitin C promoter, to visualize neurons based on mCherry fluorescence coexpressed with the shRNA.

Lentiviral Production and Infection of Cultured Neurons. The production of lentiviruses and infection of neurons with lentiviruses have been described (2). Briefly, the lentiviral expression vector and three helper plasmids [pRSV-REV, pMDLg/pRRE, and vesicular stomatitis virus G protein (VSVG)] were cotransfected into human embryonic kidney (HEK) 293T cells (ATCC) at 6, 2, 2, and 2 μg of DNA per 25-cm^2 culture area, respectively. Transfections were performed with FuGENE 6 transfection reagent (Roche) following the manufacturer's instructions. Supernatant with viruses was collected 48 h after transfection. Cortical neuronal cultures were infected at DIV4 and used for biochemical or physiological analysis at DIV14–DIV18.

Neuronal Culture. Cortical neurons were cultured from wild-type CD1 mice as described (3). Briefly, primary cortical neurons were isolated from P0-1 CD1 mice, dissociated by papain digestion, and plated on Matrigel-coated (BD Biosciences) glass coverslips. The neurons were cultured for 14–18 d in vitro in MEM (Gibco) supplemented with B27 (Gibco), glucose, transferrin, FBS, and arabinofuranosyl cytidine (Ara-C). All experiments involving handling of mice were performed in accordance with Stanford University and federal guidelines.

Calcium Phosphate Transfection of Cultured Neurons. Neuronal transfection was performed using calcium phosphate as described (2) to achieve sparse expression of the plasmids in isolated neurons that could be identified by their mCherry coexpression.

mRNA Measurements. Levels of mRNA were determined using quantitative RT-PCR. Neuronal cultures were prepared and infected in the same manner as used for recordings. RNA was collected at DIV14 using the RNAqueous kit (Ambion) according to the manufacturer's directions. The gene-specific probes were obtained from Applied Biosystems. RT-PCR reactions were set up in triplicate for each condition with 150 ng of total RNA using the LightCycler 480 reagent kit (Roche). Reactions were run and analyzed using a 7900HT Fast RT-PCR instrument (Applied Biosystems), with GAPDH serving as the internal control. In all cases, the mRNA levels of empty vector control infection were set as 1.

Electrophysiology. Electrophysiological recordings were performed essentially as described (3). Briefly, evoked synaptic responses were triggered with a 1-ms current injection (900 μA) by a bipolar nichrome wire electrode placed at a position 100–150 μm from the soma of neurons recorded. The patch pipettes were pulled from borosilicate glass capillary tubes (Warner Instruments; catalog no. 64-0793) using a PC-10 pipette puller (Narishige). The resistance of pipettes filled with intracellular solution varied between 3 and 5 MOhm. Synaptic currents were monitored with a Multiclamp 700B amplifier (Molecular Devices). The frequency, duration, and magnitude of the extracellular stimulus were controlled with a Model 2100 Isolated Pulse Stimulator (A-M Systems) synchronized with Clampex 9 data acquisition software (Molecular Devices). For current-clamp recordings, a whole-cell pipette solution was used containing (in mM) 135 K-methanesulfonate, 10 Hepes, 4 $MgCl_2$, 0.5 EGTA, 0.4 Na-GTP, 4 Na-ATP, and 10 Na_2-phosphocreatine (pH 7.4, adjusted with CsOH). For excitatory voltage-clamp recordings (eAMPA, eNMDA, mEPSC), a whole-cell pipette solution was used containing (in mM) 135 Cs-methanesulfonate, 15 CsCl, 8 NaCl, 10 tetraethylammonium-Cl, 10 Hepes, 0.2 EGTA, 0.3 Na-GTP, 4 Na-ATP, 0.1 spermine, and 10 QX-314 (pH 7.4, adjusted with CsOH). For inhibitory voltage-clamp recordings (eIPSC, mIPSC), a whole-cell pipette solution was used containing (in mM) 135 CsCl, 5 NaCl, 10 Hepes, 1 EGTA, 1 Na-GTP, 4 Mg-ATP, and 10 QX-314 (pH 7.4, adjusted with CsOH). The bath solution of ACSF contained (in mM) 140 NaCl, 5 KCl, 2 $CaCl_2$, 1.3 $MgCl_2$,10 Hepes, and 10 glucose (pH 7.4, adjusted with NaOH). Postsynaptic currents were pharmacologically isolated by adding the AMPA-R blocker CNQX (20 μM), and/or NMDA receptor blocker AP-5 (50 μM), and/or the $GABA_A$ receptor blocker picrotoxin (50 μM) to the extracellular bath solution. AMPA-R currents were performed while holding the cell at −70 mV, NMDA-R currents at +40 mV, and IPSCs at −70 mV. Spontaneous miniature postsynaptic currents (mIPSCs and mEPSCs) were monitored in the presence of tetrodotoxin (500 nM) to block action potentials, at a −60-mV holding potential. Synaptic currents were sampled at 10 kHz and analyzed offline using Clampfit 9 (Molecular Devices) software. For graphic representation, the stimulus artifacts of the current traces were removed. Miniature events were analyzed using the template matching search and a minimal threshold of 5 pA, and each event was visually inspected for inclusion or rejection by an experimenter blind to the recording condition. For spontaneous EPSC recordings, the synaptic charge transfer was integrated over 1.5 s. For current-clamp experiments, firing frequency was analyzed as the number of spikes occurring during a fixed current injection (800 ms; 50–400 pA). Paired-pulse ratios (PPR) were acquired by applying a second afferent stimulus of equal intensity at a specified time [interstimulus interval (ISI), 50–300 ms] after the first stimulus, then calculating $IPSC_2/IPSC_1$. NMDA-R decays were analyzed by fitting decay curve (peaks normalized to 1; t = 0 at the peak) with double exponentials, and calculating the weighted tau (τ_w) according to the formula: $\tau_w = \tau_f \times [I_f/(I_f + I_s)] + \tau_s \times [I_s/(I_f + I_s)]$, where I_F and I_S are the peak amplitudes of the fast and slow components respectively, and τ_F and τ_S are the respective time constants. The current–voltage (I-V) relationship of AMPA-R and NMDA-R EPSCs was measured at holding potentials from −70 mV to +40 mV. The holding potentials were later adjusted for the junction potential, which was calculated to be +10 mV.

Ca^{2+} Imaging. For Ca^{2+} imaging, neurons were loaded with Fluo-4 AM (1 μM) in ACSF plus 0.1% BSA for 45 min at 37 °C, exchanged to fresh ACSF, and allowed to equilibrate for 30 min at 37 °C before imaging. Imaging was performed on Zeiss LSM 510 confocal microscope, excitation with a 488-nm laser and collecting fluorescence passed through a 500- to 550-nm emission filter. Regions of interest were defined as neuron somatic regions that exhibited fluorescence changes in response to application of 30 μM glutamate at the end of experiment. To control for uneven loading

between neurons, amplitudes of fluorescence transients from within individual somatic regions were quantified as a fraction of the maximal fluorescence achieved in saturating (sat) Ca^{2+} concentrations determined at the end of the experiment. Fluorescent signals were quantified as the mean region of interest and expressed as $\Delta F/F_{sat} = (F - F_{min})/(F_{sat} - F_{min})$. F_{min} indicates the average fluorescence of 10 frames upon silencing of neuron activity with tetrodotoxin (500 nM). F_{sat} indicates the average fluorescence of 10 frames upon permeabilizing the cell with 10μM ionomycin in the presence of 10 mM Ca^{2+} containing ACSF. Data were analyzed as Ca^{2+} spikes/minute (typically observing one to four spikes/minute under control conditions) defined as events of synchronous network activity measured during a 1- to 2-min window after application of 50 μM picrotoxin, visualized in a field of view consisting of ~5–15 neurons (n = fields of view); $\Delta F/F_{sat}$ maximal amplitude was analyzed during this same 1- to 2-min window after application of picrotoxin (n = individual neurons). Decay time constants [T (s)] were obtained by fitting the decay curve (peaks normalized to 1; $t = 0$ at the peak) with a single exponential.

Morphological Measurements. For morphological experiments using lentivirus delivery, neurons were filled with 0.025% Lucifer Yellow (Invitrogen) in the patch pipet to obtain images of individual neurons. For transfected neuron experiments, fluorescence from mCherry-positive neurons was captured randomly for analysis. Images were acquired using a Photometrics Cascade 512B digital camera, attached to a Nikon Eclipse TE2000 inverted microscope with a 10× objective, driven by MetaMorph image-acquisition software (Molecular Devices). Images from 30 to 40 neurons per condition were reconstructed using the MetaMorph neurite application, scoring for total neurite length, neurite branch points, and soma area. For analysis of spine morphology, pyramidal neurons were imaged using a confocal microscope (Zeiss LSM 510). Z stacks of images were taken using a 63× objective, and 2D maximal projection images were reconstructed using ZEN 2009 software (Zeiss). Spine analysis was performed on secondary and tertiary dendrites to reduce variability. Spines were manually outlined, and parameters (length, head width, and density) were measured in MetaMorph software. Each neuron was analyzed across multiple dendritic branches, pooling data for 50–100 spines to calculate mean values and plot cumulative distributions.

Immunofluorescence. Neurons were fixed with 4% (wt/vol) paraformaldehyde/4% (wt/vol) sucrose for 10 min at room temperature, permeabilized with 0.1% Triton X-100 in PBS for 5 min at 4 °C, blocked with 3% (vol/vol) horse serum/0.1% crystalline grade BSA in PBS for 30 min at room temperature, and incubated with the indicated primary and secondary antibodies in blocking solution for 1 h at room temperature. The following antibodies were used in immunocytochemisty experiments: MAP2 (Sigma; 1:1,000) and synapsin (E028; 1:2,000). Neuron dendritic morphology was visualized by either MAP2 immunocytochemistry or marked by mCherry fluorescence in transfection experiments. Neurons were randomly chosen, and images were acquired using a TCS2 Leica confocal microscope with constant image settings. Z-stacked images were converted to maximal projection images and analyzed using MetaMorph Software with synapsin puncta quantified for puncta density per 10 μm of dendrite, size, and intensity.

Statistics. Data are shown as means ± SE. Statistically significant differences (Student's t test) are indicated by asterisks in the figures. Cumulative distributions were calculated by analyzing each cell recorded separately before averaging across all cells for each condition. Cumulative distribution plots were then analyzed for statistical differences by Kolmogorov–Smirnov test (www.physics.csbsju.edu/stats/KS-test.html).

1. Maximov A, Tang J, Yang X, Pang ZP, Südhof TC (2009) Complexin controls the force transfer from SNARE complexes to membranes in fusion. *Science* 323(5913): 516–521.
2. Pang ZP, Cao P, Xu W, Südhof TC (2010) Calmodulin controls synaptic strength via presynaptic activation of calmodulin kinase II. *J Neurosci* 30(11):4132–4142.
3. Maximov A, Pang ZP, Tervo DG, Südhof TC (2007) Monitoring synaptic transmission in primary neuronal cultures using local extracellular stimulation. *J Neurosci Methods* 161(1):75–87.

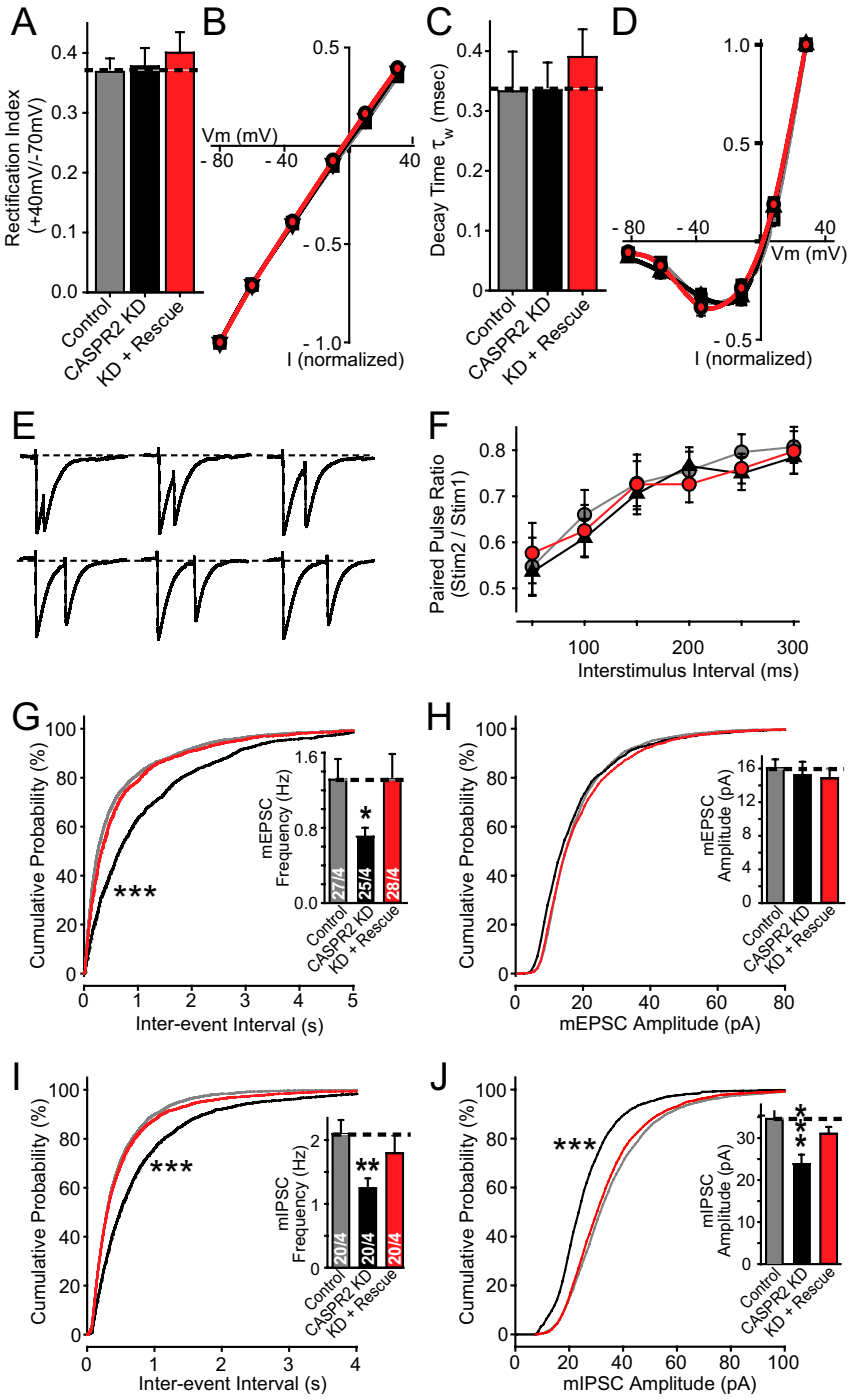

Fig. S1. Further characterization of evoked and spontaneous synaptic transmission in neurons after lentiviral CASPR2 KD. (*A–D*) Characterization of evoked AMPA-R–mediated (*A* and *B*) and NMDA-R–mediated (*C* and *D*) EPSCs measured in neurons infected with control lentivirus (control), lentivirus expressing only the CASPR2 shRNA (CASPR2 KD), or lentivirus expressing both the CASPR2 shRNA and CASPR2 rescue cDNA (KD + rescue). (*A*) Rectification index calculated as the ratio of AMPA-R EPSCs elicited with postsynaptic holding potentials of +40 mV and −70 mV (*B*) I/V curve of AMPA-R EPSCs at various holding potentials, normalized to the maximal current obtained at −70 mV. The holding potentials were later adjusted for the junction potential, which was calculated to be +10 mV. (*C*) Weighted decay constants of NMDA-R–mediated EPSCs, obtained by fitting data to a double-exponential decay curve and calculating the decay constant as a weighted tau (τ_w). (*D*) I/V curve of NMDA-R EPSCs at various holding potentials, normalized to maximal current while holding cell at +40 mV. The holding potentials were later adjusted for the junction potential, which was calculated to be +10 mV. (*E* and F) Paired-pulse experiments measuring the relative IPSC amplitude of the second to the first IPSC after application of two closely spaced stimuli (interstimulus intervals, 50–300 ms; stimulus strength was set to elicit a ∼50% maximal IPSC amplitude). Example traces for control neurons are shown (*E*), and the paired-pulse ratio ($IPSC_2/IPSC_1$) is plotted in *F*. (*G–J*) Cumulative probability plots of the mEPSC (*G*) and mIPSC interevent intervals (*I*) and amplitudes (*H and J*, respectively). Insets show mean values. Note that the small but highly significant decrease in mIPSC amplitude observed here was not detected in transfected neurons (Fig. 3) and may represent an observational bias due to the mIPSCs frequency. Data are from the experiments shown in Fig. 2*B*. Data shown are means ± SEMs; number of cells/independent cultures analyzed are depicted in the bars or listed on the graphs. Statistical significance was evaluated by Student's *t* test comparing the various test conditions to the control, except for the cumulative probability plots which were analyzed by the Kolmogorov–Smirnov test (*$P < 0.05$; **$P < 0.01$; ***$P < 0.001$).

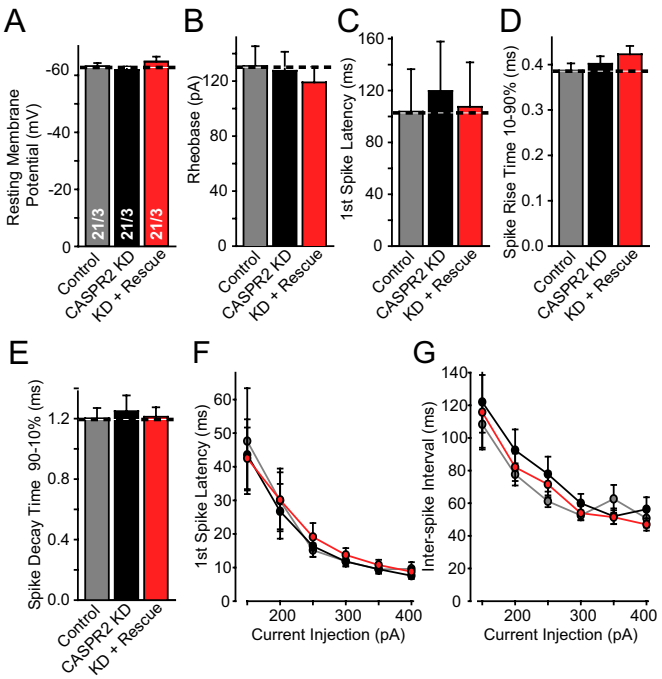

Fig. S2. Further characterization of intrinsic membrane properties and action potential generation in lentiviral CASPR2 KD neurons. (*A*) Resting membrane potentials measured in current-clamp configuration in neurons infected with control lentivirus (control), lentivirus expressing only the CASPR2 shRNA (CASPR2 KD), or lentivirus expressing both the CASPR2 shRNA and CASPR2 rescue cDNA (KD + rescue). (*B–E*) Characterization of action potential generation. In current clamp configuration, 800-ms current injections were applied in 50-pA steps to initiate generation of an action potential. The basic properties of the first action potential elicited were analyzed including: Minimum current injection (rheobase) necessary to elicit an action potential (Control: 130.9 ± 14.4 pA; CASPR2 KD: 127.5 ± 13.5 pA; Rescue: 119.0 ± 11.2 pA) (*B*), latency from start of current injection to generate first spike (Control: 103.7 ± 32.7 ms; CASPR2 KD: 119.7 ± 37.2 ms; Rescue: 107.4 ± 34.2 ms) (*C*), spike rise time (10% from baseline to 90% of maximum; Control: 0.39 ± 0.016 ms; CASPR2 KD: 0.40 ± 0.016 ms; Rescue: 0.42 ± 0.018 ms) (*D*), and spike decay time (90% of maximum to 10% from baseline; Control: 1.20 ± 0.07 ms; CASPR2 KD: 1.25 ± 0.10 ms; Rescue: 1.21 ± 0.06 ms) (*E*). (*F* and G) Current injections performed at 50-pA increments ranging from 150 to 400 pA for 800 ms were analyzed for latency to first action potential generation (*F*) and average interspike interval between multiple generated spikes during the duration of the current injection (*G*). Data shown are means ± SEMs; number of cells/independent cultures analyzed are depicted in the bars in graph *A* and apply to all graphs. Statistical significance was evaluated by Student's *t* test comparing the various test conditions to the control.

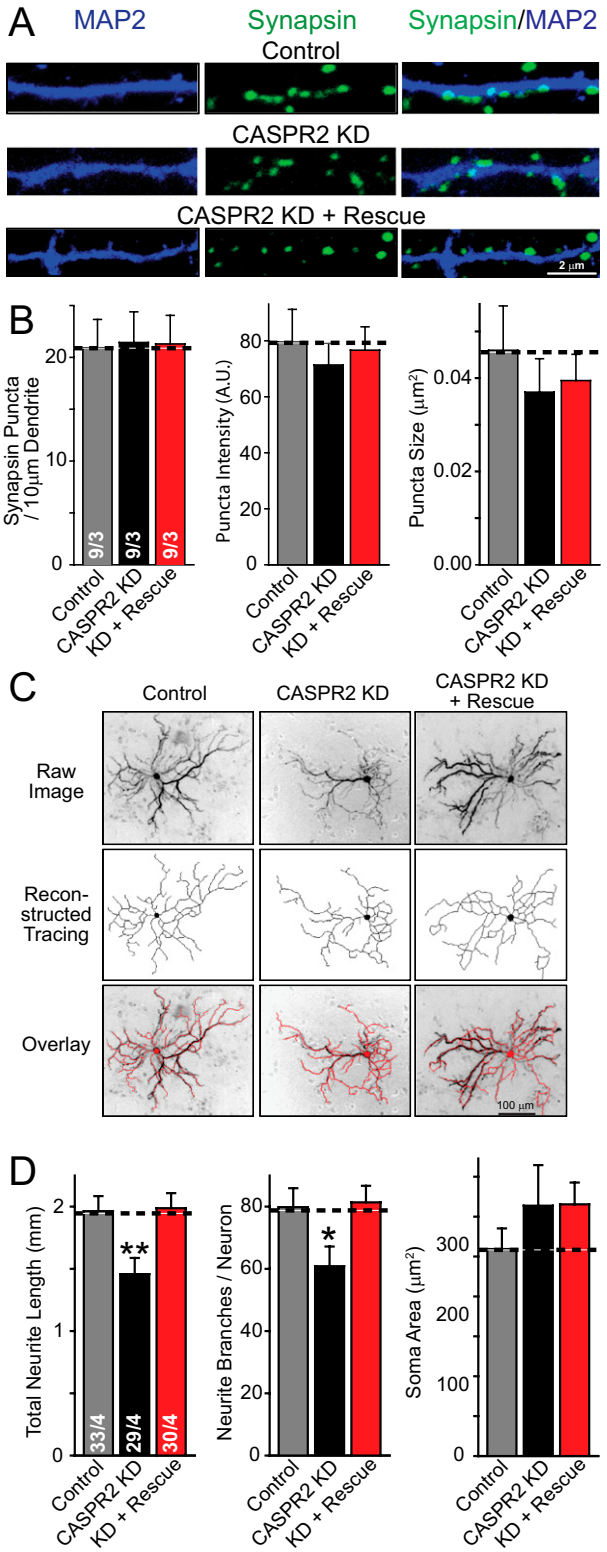

Fig. S3. Morphological characterization of neurons after lentiviral CASPR2 KD. (*A*) Representative images of immunohistochemistry experiments using antibodies against the dendritic marker MAP2 and the presynaptic terminal marker synapsin from neurons infected with control lentivirus (Control), lentivirus expressing only the CASPR2 shRNA (CASPR2 KD), or lentivirus expressing both the CASPR2 shRNA and CASPR2 rescue cDNA (KD + rescue). (*B*) Summary graphs from immunohistochemistry experiments outlined in *A*, quantifying synapsin puncta density, intensity, and size. (*C* and *D*) Representative images from neurons filled with lucifer yellow dye to analyze neuronal morphology (*C*). Neuron images were analyzed by neurite application in MetaMorph (reconstructed tracing), quantifying neurite length, branching, and soma area shown in summary graphs (*D*). Statistical significance was evaluated by Student's *t* test: $*P < 0.05$; $**P < 0.01$. Data shown in *B* and *D* are means ± SEMs; number of cells/independent cultures analyzed are depicted in the bars of a set of graphs and apply to all graphs. Statistical significance was evaluated by Student's *t* test comparing the various test conditions to the control ($*P < 0.05$; $**P < 0.01$).

Table S1. Gene families selected for analysis based on recurring association with Autism Spectrum Disorders

Gene designation	Protein name	References
CNTNAP2/CASPR2	Contactin-associated protein-like 2	1–9
CNTN3	Contactin-3	10
CNTN4	Contactin-4	11–14
GPC1	Glypican-1	15
MDGA1	MAM domain containing glycosylphosphatidylinositol anchor 1	16
MDGA2	MAM domain containing glycosylphosphatidylinositol anchor 2	16
SEZ6L2	SEZ6L2 protein	14 and 17
TMEM219	TMEM219 protein	14 and 17

1. Jackman C, Horn ND, Molleston JP, Sokol DK (2009) Gene associated with seizures, autism, and hepatomegaly in an Amish girl. *Pediatr Neurol* 40(4):310–313.
2. Alarcón M, et al. (2008) Linkage, association, and gene-expression analyses identify CNTNAP2 as an autism-susceptibility gene. *Am J Hum Genet* 82(1):150–159.
3. Arking DE, et al. (2008) A common genetic variant in the neurexin superfamily member CNTNAP2 increases familial risk of autism. *Am J Hum Genet* 82(1):160–164.
4. Bakkaloglu B, et al. (2008) Molecular cytogenetic analysis and resequencing of contactin associated protein-like 2 in autism spectrum disorders. *Am J Hum Genet* 82(1):165–173.
5. Poot M, et al. (2010) Disruption of CNTNAP2 and additional structural genome changes in a boy with speech delay and autism spectrum disorder. *Neurogenetics* 11(1):81–89.
6. Rossi E, et al. (2008) A 12Mb deletion at 7q33-q35 associated with autism spectrum disorders and primary amenorrhea. *Eur J Med Genet* 51(6):631–638.
7. O'Roak BJ, et al. (2011) Exome sequencing in sporadic autism spectrum disorders identifies severe de novo mutations. *Nat Genet* 43(6):585–589.
8. Steer CD, Golding J, Bolton PF (2010) Traits contributing to the autistic spectrum. *PLoS ONE* 5(9):e12633.
9. Nord AS, et al.; STAART Psychopharmacology Network (2011) Reduced transcript expression of genes affected by inherited and de novo CNVs in autism. *Eur J Hum Genet* 19(6):727–731.
10. Morrow EM, et al. (2008) Identifying autism loci and genes by tracing recent shared ancestry. *Science* 321(5886):218–223.
11. Fernandez T, et al. (2004) Disruption of contactin 4 (CNTN4) results in developmental delay and other features of 3p deletion syndrome. *Am J Hum Genet* 74(6):1286–1293.
12. Fernandez TV, et al. (2008) Molecular characterization of a patient with 3p deletion syndrome and a review of the literature. *Am J Med Genet A* 146A(21):2746–2752.
13. Roohi J, et al. (2009) Disruption of contactin 4 in three subjects with autism spectrum disorder. *J Med Genet* 46(3):176–182.
14. Glessner JT, et al. (2009) Autism genome-wide copy number variation reveals ubiquitin and neuronal genes. *Nature* 459(7246):569–573.
15. Sebat J, et al. (2007) Strong association of de novo copy number mutations with autism. *Science* 316(5823):445–449.
16. Bucan M, et al. (2009) Genome-wide analyses of exonic copy number variants in a family-based study point to novel autism susceptibility genes. *PLoS Genet* 5(6):e1000536.
17. Marshall CR, et al. (2008) Structural variation of chromosomes in autism spectrum disorder. *Am J Hum Genet* 82(2):477–488.

Table S2. Gene-targeting shRNA oligonucleotides used: shRNA target sequences

Gene	shRNA target sequence
CASPR1	GCCATACTGCAATCACGATAT
CASPR2	GATTAGAGCCAGAGGGAAT
CASPR3	CAGACAGTGTGGTACAATA
CASPR5	GACACAGGGCACAACTGGCAA
CNTN2	GAGTGACTGTCACTTTGGA
CNTN4	GAGAGTGTCTTCTGGGAAT
SEZ6	GCCCTTTGTCAAATACGGCAA
SEZ6L	GCTTTGAGCTCATGGGCGA
SEZ6L2	GTGTTCCTGAGAATGGTTA
GPC1	GACCGCTGCTGGAATGGAA
TMEM219	GAGTTCCACTGGTCTAGAA
MDGA1	GTCTCTTTCTTCTACCACA
MDGA2	AGGTGAAGCTAAAGAACAA

Table S3. Gene-targeting shRNA oligonucleotides used: 5′–3′ oligo sequences

Gene	5′–3′ oligo sequence
CASPR1	tcgacccGCCATACTGCAATCACGATATctcaagagaATATCGTGATTGCAGTATGGCTTTTTTggaaat
CASPR2	tcgacccGATTAGAGCCAGAGGGAATctcaagagaATTCCCTCTGGCTCTAATCTTTTTTggaaat
CASPR3	tcgacccCAGACAGTGTGGTACAATActcaagagaTATTGTACCACACTGTCTGTTTTTTggaaat
CASPR5	tcgacccGACACAGGGCACAACTGGCAActcaagagaTTGCCAGTTGTGCCCTGTGTCTTTTTTggaaat
CNTN2	tcgacccGAGTGACTGTCACTTTGGActcaagagaTCCAAAGTGACAGTCACTCTTTTTTggaaat
CNTN4	tcgacccGAGAGTGTCTTCTGGGAATctcaagagaATTCCCAGAAGACACTCTCTTTTTTggaaat
SEZ6	tcgacccGCCCTTTGTCAAATACGGCAActcaagagaTTGCCGTATTTGACAAAGGGCTTTTTTggaaat
SEZ6L	tcgacccGCTTTGAGCTCATGGGCGActcaagagaTCGCCCATGAGCTCAAAGCTTTTTTggaaat
SEZ6L2	tcgacccGTGTTCCTGAGAATGGTTActcaagagaTAACCATTCTCAGGAACACTTTTTTggaaat
GPC1	tcgacccGACCGCTGCTGGAATGGAActcaagagaTTCCATTCCAGCAGCGGTCTTTTTTggaaat
TMEM219	tcgacccGAGTTCCACTGGTCTAGAActcaagagaTTCTAGACCAGTGGAACTCTTTTTTggaaat
MDGA1	tcgacccGTCTCTTTCTTCTACCACActcaagagaTGTGGTAGAAGAAAGAGACTTTTTTggaaat
MDGA2	tcgacccAGGTGAAGCTAAAGAACAActcaagagaTTGTTCTTTAGCTTCACCTTTTTTTggaaat

Table S4. Gene-targeting shRNA oligonucleotides used: Reverse sequences

Gene	Reverse sequence
CASPR1	ctagatttccAAAAAAGCCATACTGCAATCACGATATtctcttgagATATCGTGATTGCAGTATGGCggg
CASPR2	ctagatttccAAAAAAGATTAGAGCCAGAGGGAATtctcttgagATTCCCTCTGGCTCTAATCggg
CASPR3	ctagatttccAAAAAACAGACAGTGTGGTACAATAtctcttgagTATTGTACCACACTGTCTGggg
CASPR5	ctagatttccAAAAAAGACACAGGGCACAACTGGCAAtctcttgagTTGCCAGTTGTGCCCTGTGTCggg
CNTN2	ctagatttccAAAAAAGAGTGACTGTCACTTTGGAtctcttgagTCCAAAGTGACAGTCACTCggg
CNTN4	ctagatttccAAAAAAGAGAGTGTCTTCTGGGAATtctcttgagATTCCCAGAAGACACTCTCggg
SEZ6	ctagatttccAAAAAAGCCCTTTGTCAAATACGGCAAtctcttgagTTGCCGTATTTGACAAAGGGCggg
SEZ6L	ctagatttccAAAAAAGCTTTGAGCTCATGGGCGAtctcttgagTCGCCCATGAGCTCAAAGCggg
SEZ6L2	ctagatttccAAAAAAGTGTTCCTGAGAATGGTTAtctcttgagTAACCATTCTCAGGAACACggg
GPC1	ctagatttccAAAAAAGACCGCTGCTGGAATGGAAtctcttgagTTCCATTCCAGCAGCGGTCggg
TMEM219	ctagatttccAAAAAAGAGTTCCACTGGTCTAGAAtctcttgagTTCTAGACCAGTGGAACTCggg
MDGA1	ctagatttccAAAAAAGTCTCTTTCTTCTACCACAtctcttgagTGTGGTAGAAGAAAGAGACggg
MDGA2	ctagatttccAAAAAAAGGTGAAGCTAAAGAACAAtctcttgagTTGTTCTTTAGCTTCACCTggg